CIGRE-497

2022 CIGRE Canada Conference & Expo
Calgary, Alberta, Oct.31 – Nov. 3, 2022

Large-Scale Solar PV Generation Transmission using an Energy Storage-MMC HVDC Link

N. Herath[1], S. Filizadeh[1], V. Pathirana[2]
[1]Department of Electrical and Computer Engineering, University of Manitoba
[2]Pattern Energy
Canada

SUMMARY

Large scale solar PV generation plants are typically located in remote areas such as deserts and plains, which are often several hundred kilometres away from consumers. HVDC transmission solutions are required to transmit large amounts of power over long distances; voltage source converter (VSC) based modular multilevel converter (MMC) technology has proved feasible in transmitting power while connecting into weak ac systems. Solar PV power is highly variable and could cause frequency regulation issues in weak power systems. Battery energy storage can be used to dampen the power fluctuations from solar power and the MMC with embedded storage (MMC-ES) can be used to integrate battery storage flexibly to an HVDC transmission solution. This paper discusses the applicability and advantages of using MMC-ES over a conventional MMC in transmitting highly variable solar PV power. Comparisons are done for handling loss of solar PV power, providing ancillary services, and damping power oscillations in the network with detailed simulations conducted in PSCAD/EMTDC.

KEYWORDS

Solar PV, MMC-ES, intermittent power, HVDC transmission

INTRODUCTION

Solar PV power has become increasingly affordable with low manufacturing costs [1] and government incentives. Thus large-scale solar PV plants have started to emerge in many countries. Most large-scale solar PV plants are located in remote areas such as deserts and plains due to the low cost of land, low disturbance, and clear skies. However, the population distribution, and thus the electric load, around these locations are fairly low. Load centres are typically located several hundred kilometres away, and HVDC technology has proven beneficial in transmitting large amounts of power over long distances. Solar PV power is highly variable due to the fluctuations of solar irradiance resulting from cloud movement; this could impose high fluctuations in power injections into the power system resulting in large frequency variations. This is highly undesirable and solutions to regulate power system frequency need to be implemented. Maintaining spinning reserve to dampen power oscillations has been a method of choice (which is typically based upon gas turbines), although the cost is high for the energy required to drive them. With gradually decreasing prices in batteries, battery energy storage systems (BESS) have become popular in power levelling and providing other ancillary services to power systems with a high rate of renewable penetration. Fast response, low starting time, ability to absorb and provide power, and ease of use irrespective of location, are some of the attractive qualities of BESS for providing ancillary services.

BESS have been mainly implemented based on independent converters to control the power output from battery banks [2]. Typically two-level or three-level inverters are used to convert the power. In this approach, considerable filtering at the output is required to eliminate the switching harmonics. Uneven charging and discharging could result in the battery bank due to long strings of batteries used. With this method, batteries cannot be integrated to a dc network or to a high voltage system without a scaling transformer, which could be disadvantageous in large solar PV transmission projects. As a solution, modular multilevel converters with embedded storage (MMC-ES) are introduced [3].

MMC-ES is a voltage source converter (VSC) topology that is formed with two phase arms for a given phase (Fig. 1(a)). The phase arm consists of a multivalve and an arm inductor where the multivalve is a series connection of *N* submodules (SMs). The SM is formed with a SM capacitor, a switching arrangement to insert or bypass the SM capacitor, an energy storage unit, and a filter to integrate the battery to the SM capacitor (Fig. 1(b)). The MMC-ES discussed in this paper has SMs with a half-bridge switching arrangement, a battery as an energy storage, and a bi-directional dc-dc converter as the filter. Batteries are dispersed among the SMs of the converter allowing great flexibility in charging and discharging. The converter is connected to both ac and dc networks and the batteries can be used in both networks uniformly. The large number of SMs allow the SM capacitor voltage to be a fraction of the high voltage dc link, enabling integration of batteries with ease.

This paper studies a system with two ac networks, one comparatively stronger than the other. A solar farm is connected to the weaker ac network using an overhead transmission line. The solar PV power is transmitted via a bi-pole submarine cable using MMC-ES to the stronger system. Both sending end and receiving end systems have synchronous generation with local loads. A schematic diagram of the studied system is shown in Fig. 2. Parameters of the study system are presented in Table I.

The study contains a description of a control system for the above MMC-ES study system. The ancillary controllers are shown and described in detail. A brief description of the solar PV plant modelling and control aspects are also presented. Simulations are conducted to study the impact of MMC-ES over regular MMC for loss of solar power plant generation, impact of

local feeder power measurements for ancillary services, and power smoothing capabilities for variable solar PV generation.

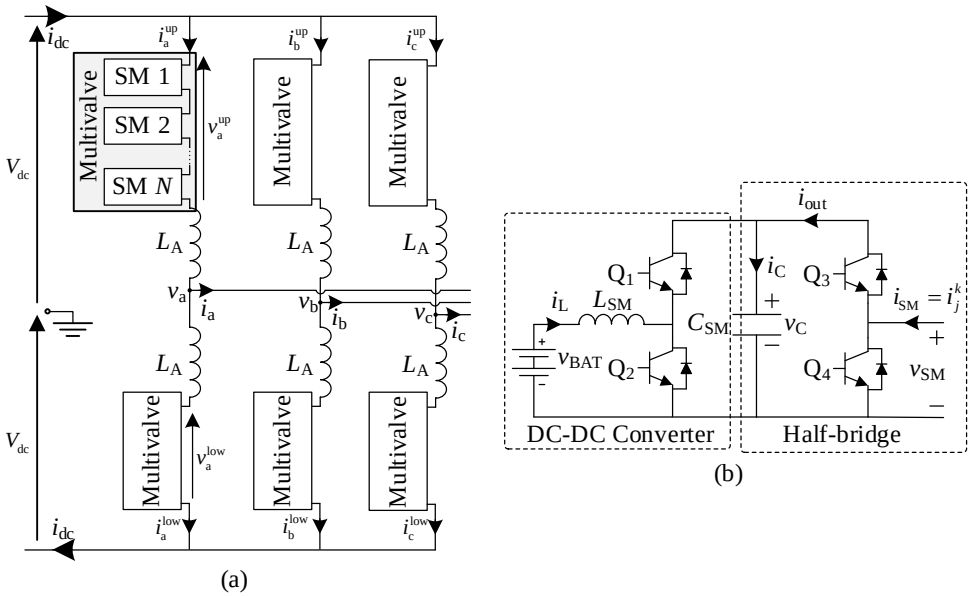

Fig. 1. MMC-ES (a) converter's schematic diagram (b) SM's schematic diagram.

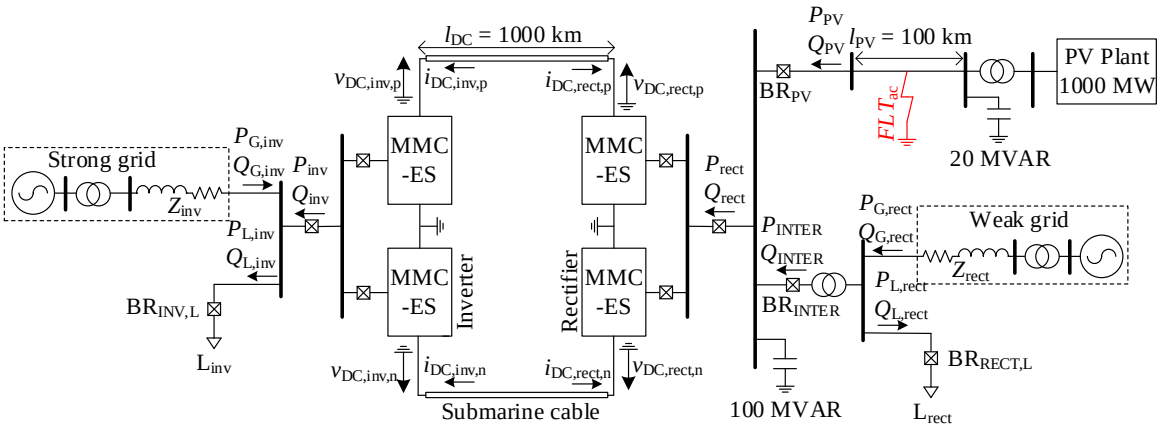

Fig. 2. Schematic diagram of the studied system.

HVDC MMC-ES AND DC CABLE

In the studied system, the power exporting converter is defined as the rectifier and power receiving converter is defined as the inverter. The MMC-ES has the ability to control ac power, dc power and the battery power. The MMC-ES's ac line currents and circulating currents are controlled using decoupled current controllers [4]. The current references for each converter are defined separately depending on the control objectives shown in Table II. The dc-c converters in each SM is controlled using an inductor current controller and with a SM average capacitor voltage controller [3], [5].

The power rating of the HVDC link requires the use of voltages of beyond 300 kV per pole to account for the IGBT switch current capability. The pole voltage of 525 kV is selected such that low conduction losses occur in the long dc transmission line. This voltage keeps in line with the Viking Link transmission system (1400 MW, 760 km, ±525 kV) [6] and the SAPEI HVDC cable (1000 MW, 420 km, ±500 kV) [7]. There are two types of HVDC submarine cables that are used in this power and voltage range: cross-linked polyethylene (XLPE) and mass impregnated insulation, non-draining compound (MIND). SAPEI project uses MIND

cables while XLPE cables were suggested for Viking Links project. The same cable used in Viking Links project is used in this study.

TABLE I
SYSTEM PARAMETERS

MMC-ES Parameters			
Power rating per pole	500 MW	Number of SMs per arm	300
SM capacitance	8.062 mF	DC voltage	±525 kV
Converter ac voltage	300 kV (ll,rms)	Arm inductance	64.4 mH
PV Plant Parameters			
PV module	KU330-8BCA	Single inverter power rating	5 MW
Inverter dc link voltage	1.2 kV	Inverter ac voltage	690 V
Total rated PV power	1000 MW	Transmission line length	100 km
Rectifier AC System Parameters			
Inertia	3.5 s	Governor droop	5%
Short circuit ratio	4 @ 75°	Rated frequency	60 HZ
Inverter AC System Parameters			
Inertia	4 s	Governor droop	5%
Short circuit ratio	8.21 @ 76.3°	Rated frequency	60 HZ
DC Cable Parameters			
Length	1000 km	Insulation	XLPE

TABLE II
CONTROL OBJECTIVES OF MMC-ES

Control parameter	Rectifier	Inverter
Decoupled q axis current reference ($i_{q,\mathrm{ref}}$)	Control ac power (P_{ac})	Control dc pole voltage ($v_{\mathrm{DC,inv}}$)
Decoupled d axis current reference ($i_{d,\mathrm{ref}}$)	Control reactive power (Q) and support ac voltage (v_{ac})	Control reactive power (Q) and support ac voltage (v_{ac})
DC component of circulating current (i_0^{circ})	DC power injected to the inverter (P_{dc})	Not controlled
SM dc-dc converters	Control the average SM capacitor voltage ($v_{\mathrm{C,avg}}$) with a feedforward term to inject SM power reference	Control dc-dc converter inductor current to obtain desired amount of power from batteries.

The protection of the MMC-ES is vital for the proper operation of the system. A simple protection system based on local measurements is implemented to detect dc voltage faults, dc current faults and ac voltage faults. Once faults are identified, the converter is blocked and converter's ac breakers are opened. Normal dc voltage is defined as between 0.9 pu and 1.1 pu. If the dc link voltage violates this range for more than 5.0 ms, a fault is detected and the converter is blocked. Similarly, if the dc current magnitude exceeds 2.0 pu for more than 5.0 ms, a fault is detected and converter is blocked.

Low voltages in the ac power system are caused by faults in the ac network. With increasing penetration of inverter-fed generation, disconnecting inverters from the network during an ac fault could lead to loss of large amounts of active power from the system, which could in turn result in frequency instability. This concern is highly relatable to distributed generation schemes such as solar PV and on-shore wind turbine interconnections. As a result, guidelines have been developed to specify the low voltage fault ride-through requirements of the inverters connected to the system. IEEE 1547 has been introduced for interconnecting distributed resources up to 10 MVA. Standards were proposed by industry such as American Wind Energy Association (AWEA) and the Western Electricity Coordinating Council (WECC) for larger generators above 20 MW. The Federal Energy Regulatory Commission (FERC), regulated these proposals and created the guideline shown in Fig. 3 for low voltage ride-through (LVRT).

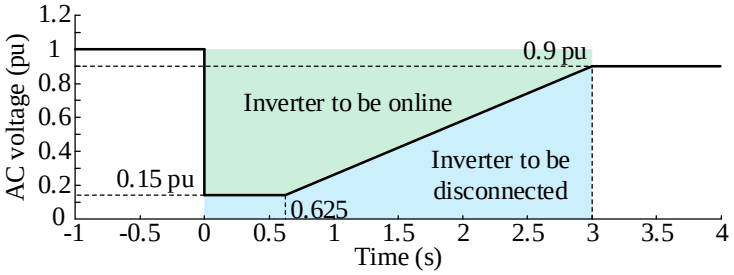

Fig. 3. Low voltage ride-through (LVRT) guideline used in the MMC-ES.

The MMC-ES is simulated as an averaged value model with blocking capability [8]. This model allows to simulate the MMC-ES converter for faults and converter blocking with high accuracy and computational efficiency.

SOLAR PV PLANT

In this study a 1000 MW solar PV plant is considered. Large-scale solar plants are typically constructed based on either a central inverter topology or a string inverter topology. String topology uses small inverters to connect PV panel strings, which allows high redundancy, with better performance at partial shading with added capital cost. Central inverters, which are rated around 5 MW, convert power of a collection of solar panel strings connected in parallel, which is used to increase the voltage and power. In this study the PV plant is modelled as a 5 MVA converter with PV panels, where the output of the inverter is scaled to match 1000 MW using a current dependent current source as shown in Fig. 4.

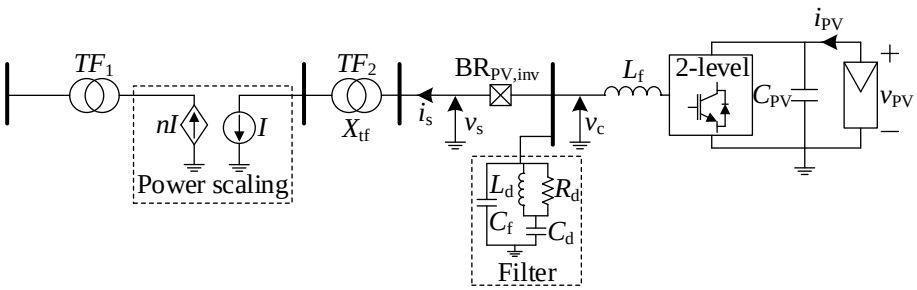

Fig. 4. Modelling of solar PV plant.

This study uses the FIMER (PVS980-58 5.0 MVA-5000kVA-L) 5 MVA inverter to design inverters for solar PV plant modelling. Simulating 200 inverters to model the 1000 MVA plant is computationally inefficient and unnecessary. In this study, a single 5 MVA converter is used with the appropriate number of PV panel modules and filter design, with its output current scaled using a current-dependent current source. This method allows to scale up the PV plant without compromising the simulation efficiency or accuracy.

MMC-ES ANCILLARY SERVICES CONTROLLERS

The variation of solar PV generation, loss of other generation, and tripping or connection of loads to the power system result in variations in system frequency and voltage. Both these parameters are expected to be within strict ranges. When a load is connected, the system frequency drops and this information could be used to increase the power output of all the generators connected to the system. A droop controller observes the frequency deviation and tries to match the power output. The rate of change of frequency (ROCOF) is also a vital parameter in the power system. The magnitude of ROCOF depends on the system inertia and the magnitude of the disturbance. A derivative controller, which provides a power reference proportional to ROCOF, can minimize the ROCOF as fast power injections can minimize the effect of the disturbance. For these controllers, system frequency is measured using phase

locked loops (PLL) and appropriate low-pass filters must be used at the frequency measurement stage in order to reject any noise present in the PLL system. System's ac voltage is dependent on the reactive power injected to the system. A droop controller that calculates the reactive power reference based on a droop setting allows to share the reactive power among the multiple sources in the system.

The main objective of the studied system is to export solar generation using MMC-ES and provide ancillary services at the respective ac networks using the embedded storage. The ancillary services controllers create power references to provide support for active power and reactive power. The rectifier controls the ac power in this study; thus the active power reference can be directly used. The inverter uses the current component related to active power (i_q) in regulating the HVDC pole voltage; thus, active power injection to ac network can be done by controlling SM battery power output. In both converters, the current component related to reactive power is used to control reactive power and a voltage droop controller can be readily used to share the reactive power support within the connected devices. Fig. 5 shows the ancillary services controllers used in both converter stations for active power and reactive power support.

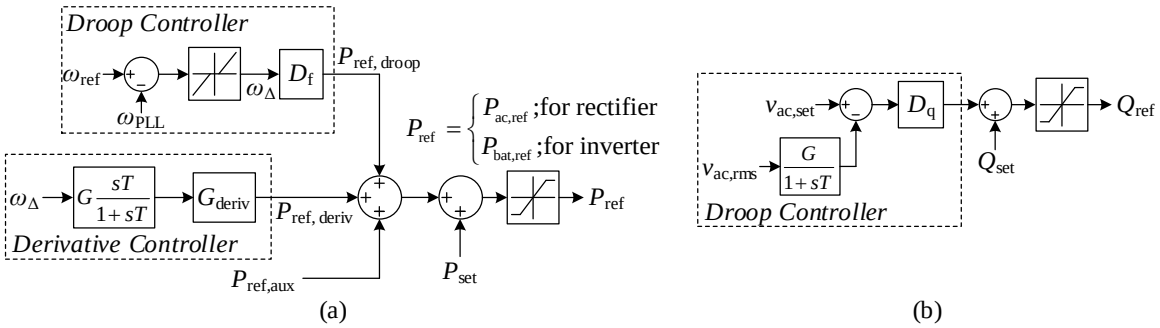

Fig. 5. Ancillary control systems (a) active power support (b) reactive power support.

In this study, the HVDC link is not expected to provide power to the rectifier-side ac system as the local generation is expected to meet the local demand. Therefore, a controller can be made using local active power measurement of PV transmission feeder to only absorb the power coming from the PV line to the rectifier MMC-ES. The rectifier will export dc power according to the operator's set point ($P_{dc,set}$) and the difference between the moving averaged PV power production ($P_{PV,MA}$) and the dc power will come from batteries in the rectifier SMs.. This ensures that there are no high variations in the rectifier-side ac network as variations from PV power are absorbed by the MMC-ES and the inverter does not observe large variations in power. A battery power set-point calculation method is also implemented in the inverter side. This controller is implemented to detect any sudden changes in dc link power and boost the battery power in the inverter end until auxiliary generators are brought online. Power set-point calculation methods for the rectifier and inverter MMC-ES are shown in Fig. 6 (a) and (b) respectively. The communication link is modelled using a sampler of constant frequency (20 kHz) and a time delay (T_1 = 1 ms). In this controller delay time constant T_2 and dc power reference gain α are selected as 1 s and 0.8, respectively.

SIMULATION RESULTS

A solid three-phase-to-ground fault is simulated at the mid-point of the solar PV transmission line. The PV line is tripped 5 ms following the fault. Studies are conducted for cases using regular MMC (labelled as Reg. MMC) and MMC-ES for dc power transmission. Fig. 7 shows the system's response following the fault for both inverter and rectifier stations. Following the fault and line tripping, large dc link voltage variations are observed for regular MMC. Protection systems observe low voltages in the system for regular MMC and trip the

MMC. The inverter end observes no frequency change following the trip of PV transmission line as battery power is able to provide the necessary frequency support.

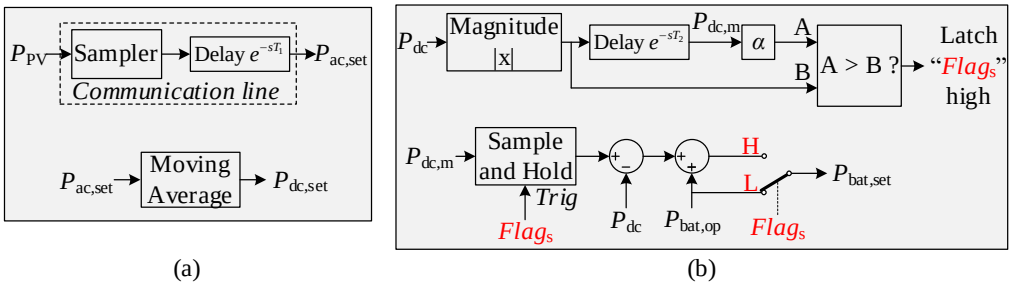

(a) (b)

Fig. 6. Power set point calculators with local active power measurements (a) rectifier (b) inverter.

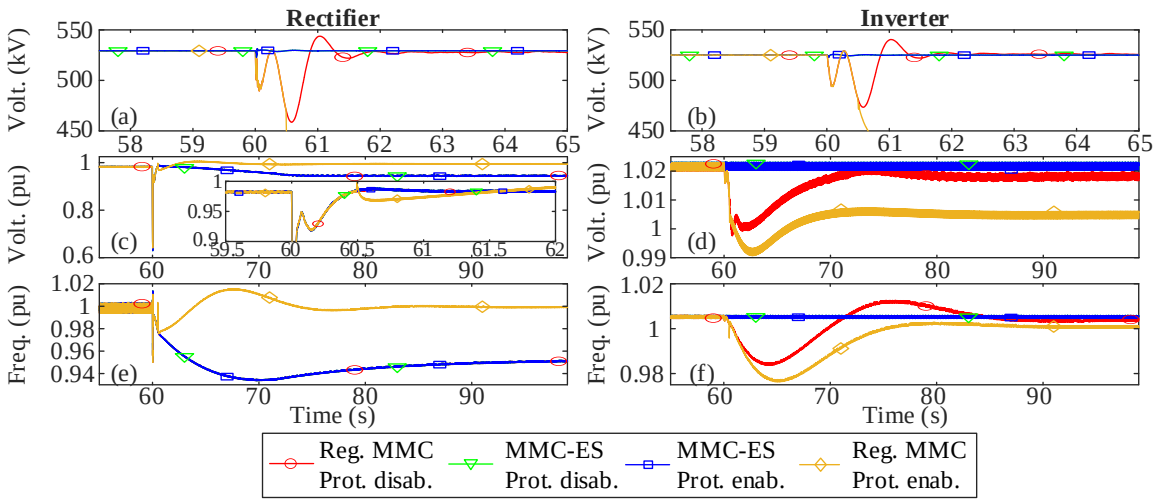

Fig. 7. Response of the dc system for a fault on ac transmission line followed by line tripping (a,b) dc +ve pole voltage, (c,d) ac rms voltage at converter, (e,f) ac system frequency-from PLL.

The impact of local P_{PV} measurement is observed in Fig. 8 with the loss of PV transmission line following a fault. Low dc voltage, converter ac voltage and frequency variations are observed with ac fault for the case with local P_{PV} measurements. Capacitor voltage is relatively impacted with the measurement of local P_{PV} (Fig. 8 (g,h)) and battery current has been ramped up rapidly (Fig. 8 (i,j)). This has helped to sustain the frequency and voltage drop and improve the network performance and quality. The power distribution of MMC-ES in Fig. 8 (k,l) shows that, batteries at rectifier end ramped the power output rapidly following the line loss with local P_{PV} measurements. The inverter end battery power are gradually ramped up to provide the lost power to the inverter side ac network. The dc line is gradually raped down to zero power as no net export of power happens from the rectifier since the PV transmission line is offline.

The test shown in Fig. 9 subjects the system to a highly variable solar irradiance profile (Fig. 9 (a)) and three different case studies are conducted and compared. Cases 1 and 2 use regular MMC to form the solar power transmission HVDC system and case 3 uses MMC-ES. Cases 1 and 3 use the power set-point calculators shown in Fig. 6; but the dc power controller for rectifier is disabled and battery power set-point calculator is disabled for cases 1 and 2 (as they are for regular MMC). For case 2, the ac power set-point ($P_{ac,set}$) is calculated directly by taking the moving average of the measured PV power injection. Case 1 and 3 observed low variations in frequency, ac voltage. The network equivalent generator power output variation is high in case 2 rectifier. Case 3, with use of MMC-ES has been able to damp out the highly variable solar power output with minimum impact to local synchronous generation while

exporting well averaged power via the dc link. The power distribution within the MMC-ES for case 3 in Fig. 9 (h,i) further shows that battery in the MMC-ES is absorbing the rapid variations in PV power without reflecting it on the ac or dc networks.

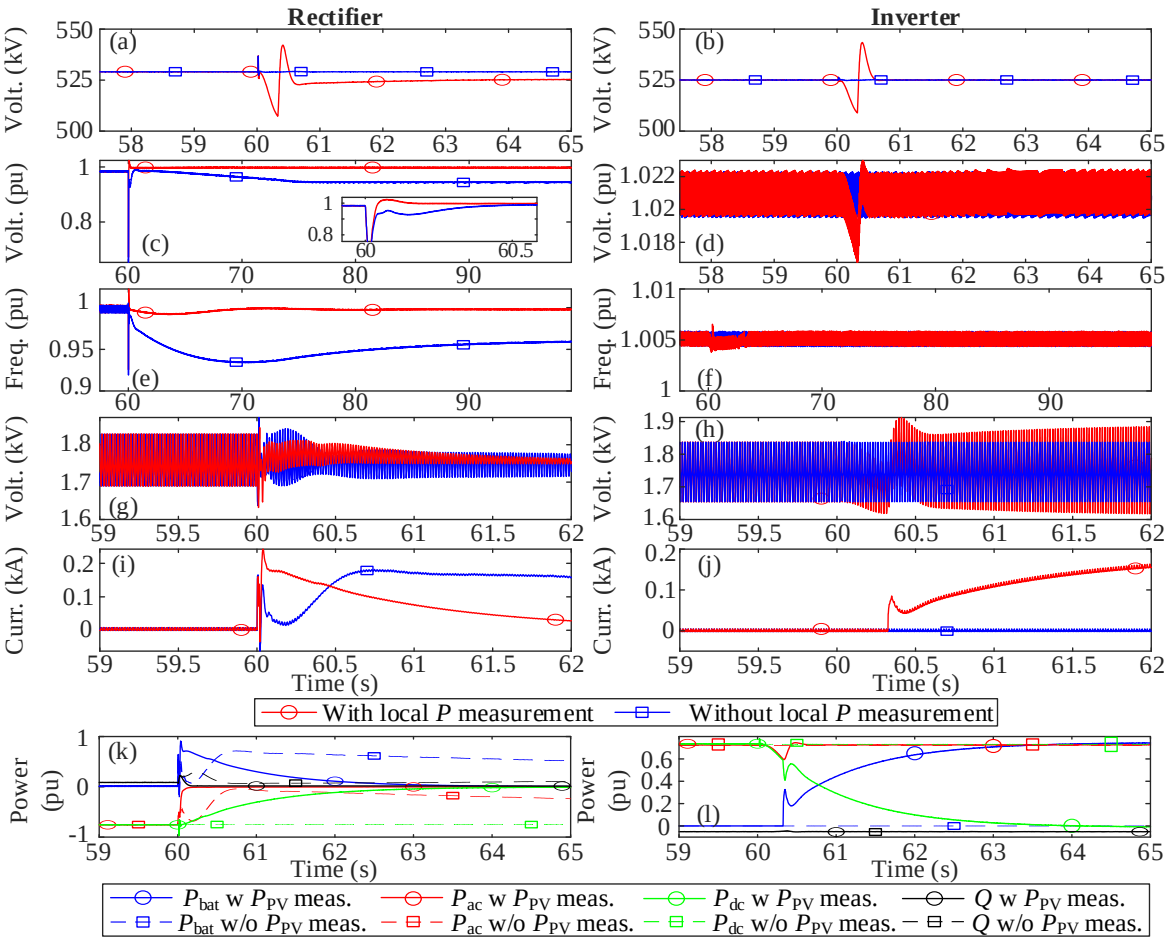

Fig. 8. Comparison of simulation data with and without P_{PV} measurement. (a,b) dc +ve pole voltage (c,d) MMC-ES ac bus voltage (e,f) ac network frequency captured by PLL (g,h) average SM capacitor voltage (i,j) average battery current (k,l) MMC-ES power distribution.

CONCLUSION

Predictability and dispatchability are key important factors in designing large-scale power plants. Large-scale solar PV are attractive forms of generation in the sense of energy cost, but are quite unpredictable and have low dispatchability. Long distance transmission of large scale power require HVDC solutions and the MMC-ES could be seamlessly introduced at this stage to increase the dispatchability and predictability of solar PV power. In this paper, detailed studies were conducted to observe the performance of an HVDC link, which is used to transmit solar PV power. Case studies with regular MMC vs MMC-ES, ancillary controller performance for MMC-ES with local PV power measurements, and performance under highly variable solar irradiance are tested. The simulation results show that the MMC-ES HVDC solutions are capable of providing attractive alterative for solar PV transmission with power system enhancement.

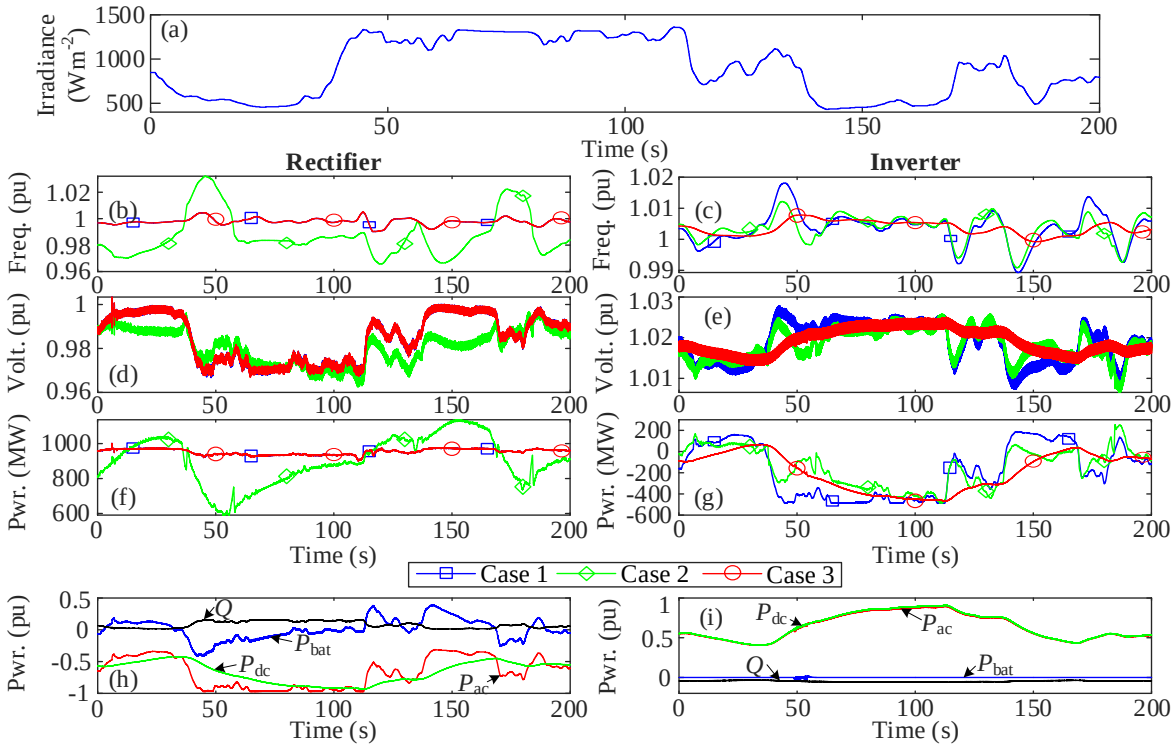

Fig. 9. System response to an irradiance profile (a) tested irradiance profile (b,c) grid synchronous machine speed (d,e) converter ac bus voltage (f,g) power output of equivalent grid (h,i) power distribution in MMC-ES for case 3.

BIBLIOGRAPHY

[1] July 26 and 2016 Noah Long Kevin Steinberger- Alum, "Renewable Energy Is Key to Fighting Climate Change," *NRDC*. https://www.nrdc.org/experts/noah-long/renewable-energy-key-fighting-climate-change (accessed Sep. 28, 2021).

[2] "PCS100 ESS," *Power Converters and Inverters*. https://new.abb.com/power-converters-inverters/power-converters-and-inverters/pcs100-ess (accessed Apr. 04, 2022).

[3] M. Vasiladiotis and A. Rufer, "Analysis and Control of Modular Multilevel Converters With Integrated Battery Energy Storage," *IEEE Trans. Power Electron.*, vol. 30, no. 1, pp. 163–175, Jan. 2015, doi: 10.1109/TPEL.2014.2303297.

[4] N. Herath, S. Filizadeh, and V. Pathirana, "Increasing Dispatchability of a PV Power Plant through Modular Multilevel Converter-Based Embedded Battery Energy Storage (MMC-EBES)," presented at the Cigre Canada Conference 2020, Toronto, Canada, Oct. 2020.

[5] T. Soong and P. W. Lehn, "Internal Power Flow of a Modular Multilevel Converter With Distributed Energy Resources," *IEEE J. Emerg. Sel. Top. Power Electron.*, vol. 2, no. 4, pp. 1127–1138, Dec. 2014, doi: 10.1109/JESTPE.2014.2342656.

[6] "Viking Link Interconnector." https://viking-link.com/ (accessed Mar. 28, 2022).

[7] "SA.PE.I. - Terna spa." https://www.terna.it/en/projects/sapei (accessed May 05, 2022).

[8] N. Herath and S. Filizadeh, "Improved Average-Value and Detailed Equivalent Models for Modular Multilevel Converters with Embedded Storage," *IEEE Trans. Energy Convers.*, pp. 1–1, 2022, doi: 10.1109/TEC.2022.3146084.